

On the fragmentation of liquid jets by neutron irradiation

Aaron Wienkers¹, David H. Sharp², Baolian Cheng² and Javier Urzay¹

¹ *Center for Turbulence Research, Stanford University, Stanford CA 94305, USA*

² *Los Alamos National Laboratory, Los Alamos, NM 87544, USA*

1. Introduction

The “holy-grail” of renewable energy — nuclear fusion — has long been sought for its clean and effectively endless potential for energy generation. One of the most studied means of achieving fusion, is inertial confinement fusion (ICF), which has been the focus of much study for the past 50 years. The fundamental goal of ICF is to compress and heat a fuel source (often solid Deuterium-Tritium, DT) into the smallest volume possible. In addition to the pertinent multi-component, and multi-phase physics dictating the implosion dynamics, a trove of hydrodynamic instabilities are known to be active throughout the implosion. These include the Rayleigh-Taylor instability on the surface of the accelerating capsule, Richtmyer-Meshkov instability due to interactions with the generated strong shocks, and general asymmetries of the fuel capsule which are amplified during the implosion. A full understanding of how these instabilities manifest in ICF is necessary in order to effectively mitigate their growth and permit a sustained thermonuclear burn.

These classical instabilities have been the topic of much study in the past few decades, but in addition to these instabilities which amplify asymmetries seeded by manufacturing the target or by the impulse itself, it has recently been shown that the presence of a fill tube, which is employed to replenish fuel, is able to seed a large-scale perturbation, as suggested by the numerical simulation results in Ref. [1]. Those simulations identified the shadowing of radiation due to the ablated SiO₂ fill-tube material as a potential perturbation influencing the implosion. It was also noticed that a radially impinging jet was generated as the fill tube is crushed and remaining DT fuel is squeezed out. Nonetheless, the results did not indicate the same degradation in yield as

observed in experiments at the National Ignition Facility (NIF) in Lawrence Livermore National Laboratory.

An aspect of the problem addressed in this investigation is the jet fragmentation over the course of the implosion and early ignition as it is bombarded with 14-MeV neutrons produced by the main fusion reactions. This mechanism in course may affect the jet penetration and mixing, and ultimately impact the formation of a hot-spot and possibility of sustained burn. It will be shown below by using a simplified model that jet fragmentation is plausible when finite compressibility effects in the liquid are considered upon the sudden heating induced by the neutron radiation.

The remainder of this manuscript is organized as follows. Estimates of characteristic scales and energies associated to the potential, full-scale jet fragmentation processes that may occur in ICF, along with a qualitative description of the neutron-energy deposition physics, are provided in Sec. 2. A simplified physical model of fragmentation, which is based on acoustic wave propagation and subsequent cavitation in the liquid as a result of the rapid energy deposition, is provided in Sec. 3. Lastly, conclusions and future work are discussed in Sec. 5.

2. Characteristic scales and energy-deposition mechanisms

As high-energy radiation bombards the ICF capsule, the Beryllium ablator vaporises, causing a back-reaction which initiates implosion of the DT capsule. Simultaneously, however, the glass fill-tube is also ablated by the radiation and crushed, ejecting a small liquid DT jet propagating radially inwards [1]. Nearly 20 nanoseconds later, as the fuel capsule has been sufficiently compressed and heated, a hot-spot forms in the centre of the imploded DT capsule, which permits fusion of hydrogen atoms and subsequent generation of high-energy 14-MeV neutrons. As these high-energy neutrons stream out of the capsule, they thermalise with the nearby DT via scattering interactions, thereby allowing a sustained thermonuclear burn. Thus they also thermalise with the impinging liquid jet, potentially generating dynamics leading to the fragmentation of the jet, which could lead to deleterious effects on the sustained nuclear burn.

For illustration purposes, consider the incidence of neutrons on the jet as a separate problem. As the 14-MeV neutrons begin to form, two disparate time-scales control the dynamics of this problem: The neutron transit and thermalisation time, and the acoustic jet-crossing time. 14-MeV neutrons

travel at about 17% of the speed of light, and so these time-scales may differ by as much as a factor of 10^5 . In particular, the slower acoustic time, which is of order R_0/c_0 , indicates that neutron-induced heating Q in the jet may be assumed to be deployed almost instantaneously and at constant volume. The resulting overpressure is of order $P'_0/P_0 \sim \beta Q/(\kappa P_0 c_v)$, where $\beta = \rho^{-1} \partial \rho / \partial T)_P$ is the volume expansivity, $\kappa = -\rho^{-1} \partial \rho / \partial P)_T$ is the isothermal compressibility, c_v is the specific heat at constant volume, ρ is the liquid density and P_0 is the initial pressure of the liquid prior to heating. In ordinary liquids, heat depositions Q of order hundreds of Kilo-Joules per kilogram as produced by 10^8 neutrons of 14-Mev energy, induce overpressures P'_0 of the order of hundreds of bars along with temperature increments $T'_0/T_0 \sim Q/(c_v T_0)$ of the order of hundreds of degrees Kelvin. These orders of magnitude, although similar to those utilized in Ref. [2] for the study of jet fragmentation in liquid films for wall protection of the fusion chamber, however appear to underestimate the characteristic conditions of the liquid jet within the fuel capsule upon heating, since the heating values in the present problem may be significantly larger due to the proximity of the jet to the fusion core.

In an ideal ICF shot, on the order of 10^{19} neutrons are generated, $\sim 10^{13}$ of which will end up traversing axially through the liquid jet. Fast neutrons are well known to only be indirectly ionising, and so they thermalise with the jet by scattering interactions, the first of which transfers on the order of $E_{\text{scatter}} \sim E_0(1 - e^{-1}) \sim 8$ MeV. Hydrogen atoms present a scattering cross-section to neutrons of $\sigma_{H,\text{scatter}} = 82$ barn, and so for the density of liquid DT near the triple point (prior to the implosion), the mean free path of scattering is $\lambda_{\text{scatter}} \sim 50 \mu\text{m}$. Using these order of magnitude estimates, and assuming that the neutrons do not scatter before reaching the jet, it is trivial to show that in total an energy density corresponding to a temperature increment $T'_0 \sim 10^8$ K is deposited into the leading $50 \mu\text{m}$ of the jet by neutron interactions. This heating value decreases with radius out of the DT capsule, where energy is transferred then by secondary scattering.

The disparate time-scales imply that hydrodynamically, the jet appears to be heated isochorically. Thus, the ‘‘instantaneous’’ energy deposition increases the jet temperature, and consequently the thermal pressure. This overpressure may be calculated using the thermal expansion coefficient and compressibility of DT; however, these values are highly nonlinear over this temperature range, and so extrapolating predicts an overpressure even higher than a few Giga-Pascals. Regardless, the analysis presented in this paper is sufficiently general for a wide range of overpressures, with caveats due to non-

linearities considered in discussion. The utilization of the present analysis to describe such extreme conditions should however be taken with caution.

Finally, it will be argued that this neutron heating results in an extremely uniform temperature and therefore pressure profile which will later be taken to be constant. Dividing the number of neutron scattering interactions randomly over the volume of the jet of length λ_{scatter} , then each 8-MeV transfer is roughly confined to a volume with length $\sim 10 \text{ \AA}$. Thus the thermal diffusion time-scale to allow this energy to uniformly spread in that volume is on the order of 10 picoseconds. Then on the acoustic relaxation time-scale, it is a very good assumption to take the overpressure as uniform.

The analysis performed below addresses the post-heating stage dominated by acoustic wave propagation in the liquid similarly to Ref. [3] albeit with additional considerations and important particularizations to the problem in question. Once the overpressure is induced isochorically and almost instantaneously by the neutron heating, an acoustic relaxation process occurs by which an expansion wave propagates into the liquid as a result of the lower ambient pressure surrounding the liquid jet. The expansion process is no longer isochoric, but involves only small density variations as prescribed by the small compressibility of the liquid. In the linear limit, the velocities induced by the expansion process are much smaller than the characteristic speed of sound in the liquid, and as a result the radial position of the liquid-gas interface can be considered to be frozen in the first approximation. The radially inwards propagating expansion wave generates large underpressures in the liquid core that may result in cavitation and, eventually, may lead to jet fragmentation. The latter stage is not studied here and requires consideration of the dynamics of the cavitation bubble as it expands radially outwards against a positive pressure gradient.

3. Formulation

As a first investigation, an infinitely long cylindrical jet will be considered to simplify the analysis and gain a bearing on the active phenomena. Homogeneity in \hat{z} can then be exploited to write the 2D fully compressible

Euler equations in the $\hat{r} - \hat{\theta}$ plane in cylindrical coordinates,

$$\frac{\partial u_r}{\partial t} + u_r \frac{\partial u_r}{\partial r} + \frac{u_\theta}{r} \frac{\partial u_r}{\partial \theta} - \frac{u_\theta^2}{r} = -\frac{1}{\rho} \frac{\partial p}{\partial r} \quad (1)$$

$$\frac{\partial u_\theta}{\partial t} + u_r \frac{\partial u_\theta}{\partial r} + \frac{u_\theta}{r} \frac{\partial u_\theta}{\partial \theta} - \frac{u_r u_\theta}{r} = -\frac{1}{\rho r} \frac{\partial p}{\partial \theta} \quad (2)$$

along with continuity,

$$\frac{\partial \rho}{\partial t} + \frac{1}{r} \frac{\partial \rho r u_r}{\partial r} + \frac{1}{r} \frac{\partial \rho u_\theta}{\partial \theta} = 0. \quad (3)$$

This system will be closed by some yet-unspecified equation of state for the liquid, $p = f(\rho)$. For an isentropic process in liquids, it can be shown that taking the liquid to be isothermal is a very good approximation, even for large variations in pressure.

We neglect surface tension as well as the inertia of the outer fluid for now, so that the kinematic and stress-free boundary conditions for the cylindrical jet applied at $r = R(\theta, t)$ are

$$p(R, \theta, t) = p_\infty \quad (4)$$

$$u_r(R, \theta, t) = \frac{DR}{Dt}(\theta, t) = \frac{\partial R}{\partial t} + \frac{u_\theta}{R} \frac{\partial R}{\partial \theta} \quad (5)$$

$$\frac{\partial r u_\theta}{\partial r}(R, \theta, t) = 0. \quad (6)$$

Only by neglecting the dynamical influence by a fluid outside of the jet can we approximate the pressure anomaly there to be 0. Nonetheless, this is a good approximation for high density ratio systems, such as for a liquid water jet in air, or for the liquid DT jet in DT vapour. Thus with no outer fluid, these dynamics are invariant to Galilean transformations, and without loss of generality, the jet may be taken to be stationary in the homogeneous direction.

This formulation must also assume that the jet remains a liquid throughout the relaxation. The presented continuum analysis fails to correctly model multi-phase phenomena such as spinodal phase decomposition which are known to dominate the dynamics after cavitation. The interested reader is referred to the molecular dynamics simulations of Blink [2], where the cavity dynamics after rapid vaporisation, and the subsequent collapse is thoroughly studied in the context of liquid metal cylinders.

Before linearising these governing equations, it will be prudent to define the characteristic scales associated with the jet geometry. The initial, and unperturbed jet radius, R_0 will give a length scale, and the velocity scale is the sound speed,

$$c_0 = \sqrt{\frac{K_0}{\rho_0}} = \sqrt{f'(\rho_0)} \quad (7)$$

where K_0 is the nominal bulk elastic modulus of the fluid at a characteristic reference state just prior to isochoric heating. Thus a characteristic sound-crossing time-scale is R_0/c_0 .

We now linearise the governing set of equations around the trivial basic state, for bulk and surface perturbations to $O(\epsilon)$. This is a good approximation when $u \ll c_0$, and when radial deviations are small compared to R_0 . The linear system is then

$$\frac{\partial u_r}{\partial t} = -\frac{1}{\rho_0} \frac{\partial p'}{\partial r} \quad (8)$$

$$\frac{\partial u_\theta}{\partial t} = -\frac{1}{\rho_0 r} \frac{\partial p'}{\partial \theta} \quad (9)$$

$$\frac{\partial \rho'}{\partial t} + \frac{\rho_0}{r} \frac{\partial r u_r}{\partial r} + \frac{\rho_0}{r} \frac{\partial u_\theta}{\partial \theta} = 0. \quad (10)$$

It can also be shown that evaluating the boundary conditions at $R(\theta, t)$ is a quadratic correction, and so evaluation at R_0 is sufficient. The boundary conditions are then

$$p'(R_0, \theta, t) = 0 \quad (11)$$

$$u_r(R_0, \theta, t) = \frac{\partial R}{\partial t} \quad (12)$$

$$\frac{\partial u_\theta}{\partial r}(R_0, \theta, t) = -\frac{u_\theta}{R_0}. \quad (13)$$

Linearising the equation of state about p_0 gives $p' = \rho' c_0^2$. Finally, combining equations (8)-(10) gives the 2D linear acoustic equations for a cylindrical jet with a free surface:

$$\frac{\partial^2 p'}{\partial t^2} = c_0^2 \nabla^2 p' = c_0^2 \left[\frac{1}{r} \frac{\partial}{\partial r} \left(r \frac{\partial p'}{\partial r} \right) + \frac{1}{r} \frac{\partial}{\partial \theta} \left(\frac{1}{r} \frac{\partial p'}{\partial \theta} \right) \right]. \quad (14)$$

This formulation, (14), is now valid only for low Mach flows, where $|u| \ll c_0$, so that the nonlinear terms remain small. This is an increasingly good

approximation in liquids even for quite extreme pressure fluctuations (less than $O(K_0)$), but it will still be shown that the density anomaly remains small throughout the relaxation compared to the reference density.

4. Results

A number of instability modes viable in small-scale liquid jets have been identified, and their relevance will be discussed in light of the time-scale for each mechanism to grow. For this study, both droplet formation and cavitation will be assumed to be direct routes to fragmentation, although this assumption has been more closely studied using molecular dynamics simulations by Blink [2].

4.1. Capillary Instability

The most obvious instability inflicting small-scale cylindrical jets with a distinct liquid interface is the Rayleigh-Plateau (capillary) instability. Although it is physically decoupled from the direct effects of neutron heating of the jet, there is still a short period between jet formation and the initial fusion event generating 14-MeV neutrons. Nonetheless, it will be apparent that on the time-scales dominating the dynamics of this problem, the capillary instability is much too slow. This instability is inherently axisymmetric, with the most unstable wavenumber inflicted being $O(1/R_0)$ (in fact, $\lambda_{\max} = 0.11R_0$). This implies the e-folding time-scale is

$$\tau_{\text{RP}} \sim \sqrt{\frac{\rho_0 R_0^3}{\gamma}} \quad (15)$$

where γ is the surface tension of the DT liquid-vapour interface. The ratio of this break-up time by the Rayleigh-Plateau instability compared to the sound crossing time is

$$\frac{\tau_{\text{RP}}}{\tau_{\text{sc}}} \sim \sqrt{\frac{R_0 K_0}{\gamma}}. \quad (16)$$

A typical value for the ratio K_0/γ is on the order of 10^{10} m^{-1} , and so the capillary instability may be safely disregarded for jet radii greater than a few nanometres when dominant dynamics also occur on the acoustic time-scale.

4.2. Richtmyer-Meshkov Instability

The impulsively accelerated limit of the Rayleigh-Taylor instability, the Richtmyer-Meshkov instability (RMI), preys on small potential energy variations in a density interface when impulsively accelerated, depositing large amounts of vorticity at the interface. This may be observed, for example, when a flat pan of water impacts the ground, or in supernovae, but has also been well studied in ICF applications as the capsule is impulsively accelerated inwards [4]. This instability is likewise active at the surface interface of the liquid jet because it is similarly impulsively accelerated upon heating (shown in Figure 4 of §4.3.2). For negative Atwood numbers, the so-called indirect inversion RMI [4] sees a momentary decay followed by a phase shift and subsequent linear growth,

$$\sigma_{RMI} = Ak\Delta u_r. \quad (17)$$

Thus for $|A| = 1$, corresponding to $\rho_\infty = 0$ and $\Delta u_r = p'_0/(\rho_0 c_0)$, the time-scale for the most dynamically disruptive wavenumber is

$$\tau_{RMI} \sim \frac{R_0 \rho_0 c_0}{p'_0}. \quad (18)$$

Thus for $p'_0 \ll \rho_0 c_0^2$, the Richtmyer-Meshkov instability will occur on a time-scale many times the acoustic time, and so may be safely disregarded for now.

4.3. Pressure Relaxation after Isochoric Heating

As shown in §2, the time-scale of neutron heating is much shorter than the acoustic time, and so the effect of neutrons heating the jet may, to a first approximation, be taken as uniform isochoric heating. Thus at $t = 0$, the jet is modelled as experiencing a sudden overpressure which (in order to satisfy the pressure boundary, (11)) subsequently generates a tensile rarefaction wave propagating radially inwards. As the rarefaction wave amplifies, the liquid experiences increasingly low pressures, and may eventually cavitate. However, in the absence of vapour nucleation points such as boundary walls, pure liquids can remain in phase at pressures well below their vapour pressure. Liquids in this *metastable* state are even known to withstand negative (tensile) pressures before cavities finally arise spontaneously and nonuniformly due to thermal fluctuations. This limit of metastability, is

the spinodal pressure limit [5], and will be used in lieu of the vapour pressure as an indicator of impending cavitation.

These dynamics all occur on the acoustic time-scale, and therefore are the first behaviours that are necessary to fully understand. Cavitation following pressure relaxation is thus argued to be the first mechanism in the evolution of the ICF implosion which may cause fragmentation. In this case, any other dynamics inflicting this basic state on slower time-scales are wholly irrelevant, as the base state would by that time have been sufficiently modified by the cavitation event.

The dynamics after cavity formation have been previously investigated both with an integrated continuum multiphysics program [6], and more closely using molecular dynamics simulations [2]. Specifically, Blink [2] found that, unlike cavitation bubbles that form in the bulk of a quiescent fluid, cavities in this relaxing system are robust and long-lived. Hassanein and Konkashbaev [6] was concerned with the dynamics of centrally heated liquid metal spallation blanketing jets [7], but made the observation that a subsequent strong outward-propagating shock wave is generated as the energy stored in the tensile stress of the liquid is suddenly released at cavitation.

These two findings suggest that cavity formation would be detrimental to the coherency of a cylindrical jet, ultimately leading to fragmentation. Thus in the following, we will demonstrate the inevitability of an idealised geometry to cavitate, and suggest possible physical mechanisms which might mitigate this in reality.

4.3.1. Characteristic Solution for Spherical Geometry

The linear acoustic equations (14) may instead be formulated in spherical coordinates, which along with assuming axisymmetry, a great simplification can be made which allows an analytic solution by the method of characteristics. This simplified spherically-symmetric linear acoustic equation is

$$\frac{\partial^2(rp')}{\partial t^2} = c_0^2 \frac{\partial^2(rp')}{\partial r^2}. \quad (19)$$

Thus by direct analogy to the 1D Cartesian linear acoustic equation, admitting the d'Alembert wave solution with acoustic invariants,

$$F_c = \frac{1}{2} \left(\frac{u_0}{c_0} + \frac{p'_0}{\rho_0 c_0^2} \right) \quad (20)$$

$$G_c = \frac{1}{2} \left(\frac{u_0}{c_0} - \frac{p'_0}{\rho_0 c_0^2} \right) \quad (21)$$

the spherical invariants become $F_s = rF_c$ and $G_s = rG_c$.

Thus with initial conditions corresponding to an instantaneously heated drop,

$$\mathbf{u}(r, \theta, t) = 0 \quad (22)$$

$$p'(r < R_0, \theta, t) = p'_0 > 0 \quad (23)$$

$$p'(r \geq R_0, \theta, t) = 0, \quad (24)$$

it is easy to show that $F_s = -G_s$, and so the characteristic solution for pressure is

$$p'(r, t) = \frac{r + c_0 t}{2r} f(r + c_0 t) + \frac{r - c_0 t}{2r} f(r - c_0 t) \quad (25)$$

where here r is a spherical radius. The function, $f(\xi)$ is defined so as to satisfy the boundary condition at R :

$$f(\xi) = p'_0 \quad \text{for } \xi < R_0 \quad (26)$$

$$f(\xi) = \left(1 - \frac{2R_0}{\xi}\right) p'_0 \quad \text{for } \xi \geq R_0. \quad (27)$$

The term of interest in (25) is the first term on the right-hand side, which describes the relaxation wave propagating inwards from the boundaries, and which is produced when enforcing the pressure anomaly to be 0 at the boundary. This is seen in Figure 1, which shows the relaxation wave moving from right to left with time. The radially outward-propagating wave is still necessary to momentarily prevent a singularity at $r = 0$, by exactly cancelling with the first term. Nonetheless, it is immediately apparent that once this symmetry breaks in equation (25), (i.e. when $c_0 t \geq R_0$, so that $p' = 0$ there) then a singularity appears at $r = 0$.

The extension of this characteristic solution to cylindrical geometry is not as trivial as again modifying the invariants. Nevertheless, a characteristically ardent reader may show that

$$p'(r, t) = \int_r^\infty \frac{r_s + c_0 t}{2\sqrt{r_s^2 - r^2}} f(r_s + c_0 t) dr_s + \int_r^\infty \frac{r_s - c_0 t}{2\sqrt{r_s^2 - r^2}} f(r_s - c_0 t) dr_s \quad (28)$$

by integrating out the spherical radius r_s from the solution (25), from $z = -\infty$ to $+\infty$. Here now r is the cylindrical radius, and $f(\xi)$ must be carefully chosen again to ensure that $p'(R_0, t) = 0$ using the cylindrical radius. Similarly to the spherical argument, it is evident again that a singularity will form when asymmetries in the terms tending towards infinity are not cancelled when $t = R_0/c_0$.

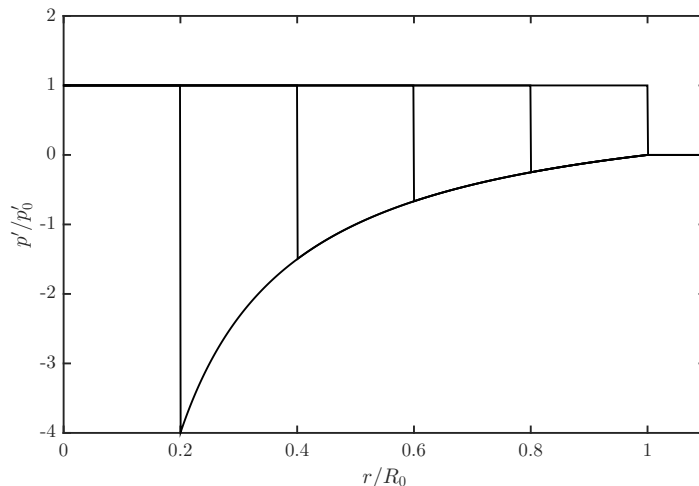


Figure 1: Nondimensional pressure anomaly for the relaxation of an isochorically heated spherical drop. Shown here (from right to left) at $t = 0, 0.2, 0.4, 0.6, \& 0.8$.

4.3.2. Series solution for Cylindrical Geometry

Although integrating out the spherical component to get a characteristic solution for cylindrical geometry gives some intuition into the asymptotic behaviour, in practice the form of the function $f(\xi)$ is not straightforward, and must be computed numerically either way. Thus, a solution of the linear acoustic equation in cylindrical coordinates (14) by an expansion in eigenmodes will prove more useful, in addition to permitting further extension to 2D with azimuthal variations.

Proposing an expansion in the form $p'(r, t) = \hat{p}(r) \exp(-i\omega t)$, then the governing equations are reduced to the ODE,

$$\frac{d^2 \hat{p}}{dr^2} + \frac{q}{r} \frac{d\hat{p}}{dr} + \frac{\omega^2}{c_0^2} \hat{p} = 0. \quad (29)$$

This differential eigenvalue problem has solutions in the form of Bessel functions, with corresponding eigenvalues given by $\omega_n = c_0 j_{0,n} / R_0$, where $j_{0,n}$ is the n^{th} zero of the 0th order Bessel function, $J_0(r)$. Thus in nondimensional variables using the jet radius and sound-crossing time, the series solution may be written as

$$p'(r, t) = \sum_{n=1}^{\infty} \beta_n J_0(j_{0,n} r) e^{-ij_{0,n} t}. \quad (30)$$

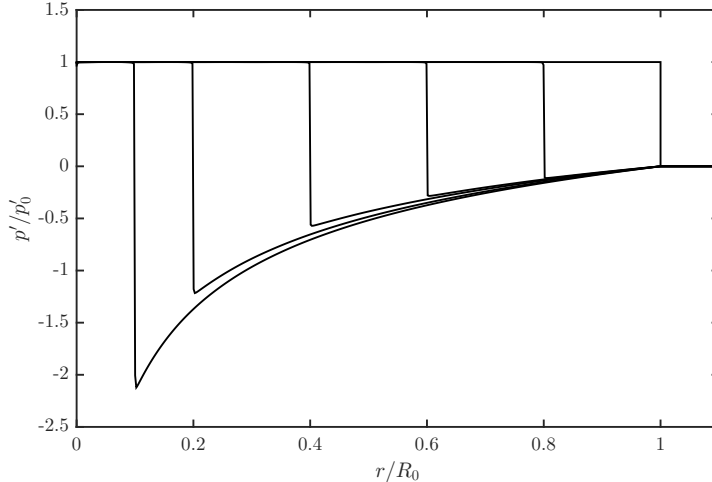


Figure 2: Nondimensional pressure anomaly for the relaxation of an isochorically heated cylindrical jet. Shown here (from right to left) at $t = 0, 0.2, 0.4, 0.6, 0.8, \& 0.9$.

The coefficients, β_n , of the eigenfunctions are again specified by a transform of the initial condition into the Bessel basis. Using the initial conditions, (23) - (24), this coefficient may be computed analytically as

$$\beta_n = \frac{2}{j_{0,n} J_1(j_{0,n})}. \quad (31)$$

This series solution was computed using the first $N = 100$ modes in the series, and is presented in Figure 2. In comparison to the spherical geometry relaxation, it is interesting to note that the pressure anomaly continues to decrease in time at a given radius for the cylindrical jet. This is best interpreted as the weak spherical rarefaction waves at $z = \pm\sqrt{c_0^2 t^2 - r^2}$ from the characteristic integral solution, (28), still arriving to the radius r , even after the initial rarefaction wave has passed. Additionally, as predicted, the removal of the additional dimension of focussing present in the spherical geometry reduces the pressure anomaly by about a factor of 2, but nonetheless does not remove the singularity in the solution.

The velocity profile was also computed using the complement of the radial linear acoustic pressure equation (14), and is presented in Figure 3. The fluid bulk velocity is seen to be quite supersonic in the majority of the jet; however, as is the case in our hyperbolic world, the rarefaction front still only

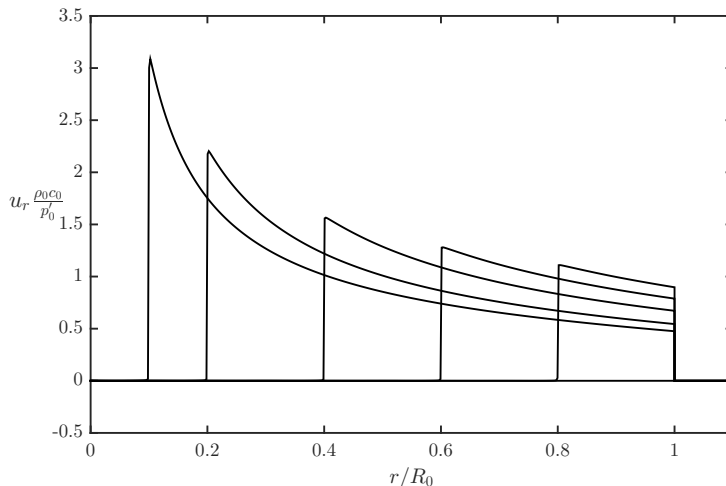


Figure 3: Nondimensional radial velocity profile for the relaxation of an isochorically heated cylindrical jet. Shown here (from right to left) at $t = 0, 0.2, 0.4, 0.6, 0.8, \& 0.9$.

advances at speed c_0 . An interesting observation from this velocity profile comes from computing the radial acceleration of the jet surface (shown in Figure 4). There is an integrable singular surface acceleration at the time of energy deposition, yet after this period of strong acceleration for $t < 1/2$, the surface experiences weak deceleration for $t > 1/2$. It is this acceleration which would allow Rayleigh-Taylor-unstable azimuthal waves to grow on the jet surface.

Thus in the highly idealised perfectly axisymmetric spherical and cylindrical geometry, cavitation (and consequently fragmentation) is inevitable, regardless of how low the liquid vapour pressure is or even how small the thermal overpressure is! In this theory, the cavitation bubbles are expected to arise in a cylindrical shell at a radius which is only weakly dependent on the spinodal pressure and initial overpressure.

To test the validity regime of the previous linear formulation, a concrete example will now be developed using a liquid water jet to build intuition into this phenomenon.

4.3.3. Liquid Water Jet

As much is yet unknown about the exact state of the DT jet produced in an ICF implosion, as a first demonstration, we will consider a small liquid water jet. For example, if we start with a liquid jet at 20°C and atmospheric

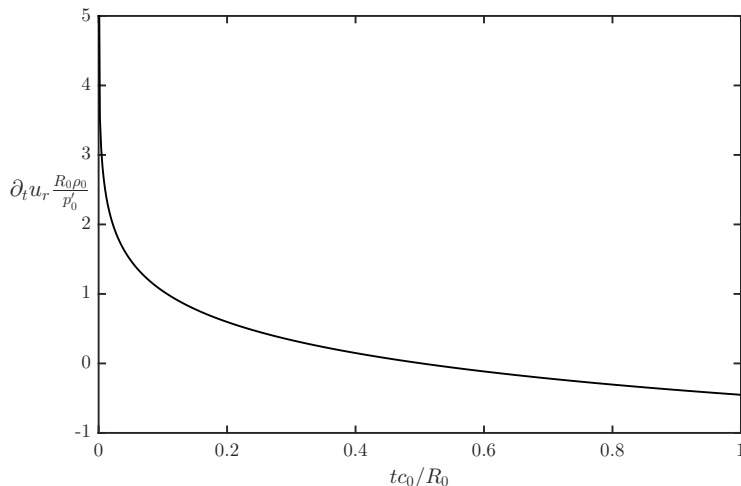


Figure 4: Nondimensional outward radial acceleration of the cylindrical jet surface in time, from $t = 0$ to the singular point at $t = 1$.

pressure, and then instantaneously heat it to 100°C , then an overpressure of nearly 36 MPa is produced (the ratio of the expansivity to isothermal compressibility at 20°C is $\sim 4.6 \cdot 10^5 \text{ Pa K}^{-1}$). At this new temperature, although the vapour pressure is 101 kPa, the spinodal limit at which spontaneous cavitation occurs is -160 MPa . In dimensionless units, $p'_s/p'_0 = -4.4$, so that using Figure 2, cavitation is guaranteed at $r = 0.04$. At the cavitation point, our presented analysis breaks down; however, just before this, $\rho' = p'_s/(\rho_0 c_0^2) = 7.3 \cdot 10^{-2}$, which is still small enough so that the linear acoustic approximation remains valid.

4.3.4. Mechanisms Mitigating Cavitation

Without a known equation of state of the liquid DT at extreme temperatures, the nonlinear solution of the governing equations cannot be found. Nonetheless, it is known that the nonlinear terms would produce a dispersive effect in the relaxation wave, enough so to possibly avoid cavitation altogether. With a specified equation of state, then the course of relaxation will depend on the magnitude of the overpressure, and could not be presented as a generalised solution as in Figure 2.

The presented analysis is thus in a sense the worst case scenario for cavitation, as the perfect symmetry means that the acoustic energy — however small — will inevitably be focussed into a point. This has led us to the non-

physical conclusion that cavitation is inevitable in an isochorically heated cylinder. Asymmetries, either in the bulk via nonuniform heating, or by azimuthal surface perturbations are expected to reduce the focussing effect, and may ultimately avoid cavitation.

Finally, if we relax the assumption of an outer vacuum, so that the outer fluid is dynamically important, energy may now be lost across the jet surface during relaxation. Nonetheless, this amounts only to an effective decrease in the initial overpressure, and so must still be paired with another means of avoiding cavitation above.

5. Conclusion and Future Work

We have shown that among the many hydrodynamic instabilities that may be active in small-scale liquid jets, the fastest mode to jet fragmentation is through cavitation during pressure relaxation. In the investigation of the relaxation after isochoric heating, we found that axisymmetric models contain an unphysical singular point (or line) along the axis. Although this is a valid solution of the governing equations, it is a sole consequence of the perfect symmetry in the problem. Thus to gauge how close to reality this conclusion is, further investigation into the focussing effects during pressure relaxation in a 2D, non-axisymmetric model is necessary.

Moreover, additional details clarifying the relative times of the jet formation and first generation of high-energy neutrons are required to ensure that the heating of the jet by 14-MeV neutrons — an event which by definition occurs after fusion has begun — indeed dominates the dynamical evolution of the jet. Thus it is yet to be convincingly shown that the ability for a nuclear burn to be sustained is impacted by the isochoric jet heating which occurs *after* the hot-spot forms, and whose dynamics are quite significantly slower.

Finally, the global stability of the jet must be considered further. Still, the dynamics of the plume generated due to jet deceleration in the ICF capsule radial pressure gradient is an important remaining avenue of investigation.

References

- [1] J. Edwards, M. Marinak, T. Dittrich, S. Haan, J. Sanchez, J. Klingmann, J. Moody, The effects of fill tubes on the hydrodynamics of ignition targets and prospects for ignition, *Physics of Plasmas* 12 (2005) 056318–9.
- [2] J. A. Blink, Fragmentation of Suddenly Heated Liquids, Ph.D. thesis, University of California, Davis, 1984.
- [3] X. M. Chen, V. E. Schrock, The pressure relaxation of liquid jets after isochoric heating, *Fusion Science and Technology* (1991).
- [4] J. D. Lindl, R. L. McCrory, E. M. Campbell, Progress toward Ignition and Burn Propagation in Inertial Confinement Fusion, *Physics Today* 45 (1992) 32–40.
- [5] R. J. Speedy, Limiting forms of the thermodynamic divergences at the conjectured stability limits in superheated and supercooled water, *The Journal of Physical Chemistry* 86 (1982) 3002–3005.
- [6] A. Hassanein, I. Konkashbaev, Modeling and simulation of fragmentation of suddenly heated liquid metal jets (2001).
- [7] R. Abbott, S. Pemberton, P. F. Peterson, G. P. Sun, P. Wright, R. Holmes, J. Latkowski, R. Moir, K. Springer, Cylindrical liquid jet grids for beam-port protection of thick-liquid heavy-ion fusion target chambers, *Fusion Technology* 39 (2001) 732–738.